



Original scientific paper

Theoretical study on quantum transport of carbon nanotubes for detecting toxic molecules: The role of dopants

Yoshitaka Fujimoto✉

Department of Applied Chemistry, Kyushu University, Moto-oka, Nishi-ku, Fukuoka 819-0395, Japan

Corresponding author: ✉fujimoto.yoshitaka.093@m.kyushu-u.ac.jp

Received: January 20, 2022; Accepted: March 1, 2022; Published: March 15, 2022

Abstract

We study the effects of dopant atoms on quantum transport and adsorption properties of environmentally harmful (CO_2), toxic (CO) and common (O_2 and N_2) molecules of carbon nanotubes (CNTs) based on the first-principles electronic structure and quantum transport study. It is found that CO and O_2 molecules can bind on the boron (B)-doped (14,0) CNTs with relatively large adsorption energies and short binding distances in air. We also studied the quantum transport of B-doped (14,0) CNTs for the adsorption of the molecules. The quantum transport properties of the CNTs are found to be sizably varied by the introduction of a dopant atom and the adsorption of the molecules. The nature of the variation of the quantum conductance induced by the doping as well as the molecular adsorption is discussed, and the possibility to individually detect toxic CO and common O_2 molecules under low bias voltages is also discussed.

Keywords

First-principles electronic transport theory; conductance; doping; molecular/gas sensors

Introduction

Carbon nanotubes (CNTs) have attracted much attention as potential electronic device materials to be used in field-effect transistors, sensors, etc. since they show excellent transport properties such as high carrier mobility and large current density [1,2]. Nanotube-based molecular and/or gas sensors have been demonstrated with a fast response time and high sensitivity at room temperatures [3-7]. In molecular sensors, target molecules can be detected by gauging the change of conductivity of the nanotubes induced by the adsorption of molecules [3,4,8-12].

First-principles density-functional calculations suggested that a pristine CNT as well as graphene does not chemically but rather physically bind with several molecules such as O_2 and NO_2 , and it is surmised that the reactivity of the pristine CNTs to adsorbates is weak [13-15]. Therefore, the electronic structures, as well as the transport properties of the pristine CNTs, are not changed largely by the adsorption of molecules [16]. Doping with heteroatoms often modifies their electronic

structures as well as improves the chemical reactivity to the adsorbates around the dopant atoms [17]. Boron and nitrogen are good dopants for carbon-based materials since they are neighboring atoms to carbon [18,19]. Actually, it is shown that the adsorption energies of H atoms and NH₃ molecules on B-doped and N-doped CNTs are larger than those on pristine ones [20,21]. Moreover, it is reported that the adsorption energies of various molecules on the B-doped graphene and CNTs are enhanced than those on the N-doped ones [10,17]. Several theoretical studies for electronic transports of CNTs and graphene decorated by doping with heteroatoms and the introduction of defects have been reported [8,22], and however, their theoretical calculations are performed under the zero defect-density limitation. The transport properties of doped CNTs with a finite defect density have to be considered to understand the effects of the dopant atoms and the molecular adsorption on the transport properties under more realistic situations.

In this paper, we report the doping effect with a heteroatom and the adsorption effects of environmentally harmful (CO₂), toxic (CO) and common (O₂ and N₂) molecules in air on the energetics and the quantum transport of B-doped (14,0) CNT based on first-principles electronic-structure and quantum transport calculations. It is found that CO and O₂ molecules are adsorbed on the B-doped CNTs in the air with relatively large adsorption energies. It is also found that the quantum transport properties of nanotubes change by the introduction of the dopant atom and the adsorption of the molecules. Scanning tunneling microscopy (STM) images for the adsorption of the molecules on the B-doped (14,0) CNTs are demonstrated, and it is found that the B-atom dopant and the CO and O₂ molecules can be distinguished from one another in the STM images.

Methodology

First-principles electronic-structure calculations have been performed within the density-functional theory (DFT) [23]. The exchange-correlation effects are treated by the local density approximation (LDA) parameterized by Perdew and Zunger [24-26]. The norm-conserving Troullier-Martins pseudopotentials are used to describe the interactions between the ions and the valence electrons [27]. For the calculation of the adsorption energy of the O₂ molecule on the B-doped CNTs, we use the local-spin-density approximation.

We here use the B-doped (14,0) CNT, which has two-unit cells for the calculations of energetics and electronic structures regarding the adsorption of various molecules. To avoid any interactions between neighboring tubes, the supercell lattice constant of as long as 24 Å (1 Å = 0.1 nm) along the direction perpendicular to a tube direction is used. The wave functions in the Kohn-Sham equations are expanded using the plane-wave basis set with the cutoff energy of 50 Ry (1 Ry = 8.72 × 10⁻¹⁸ J) [28]. One-dimensional Brillouin-zone integration is performed with 12 k-point samplings. The atomic geometries are optimized until the maximum values of the Hellmann-Feynman forces acting on all atoms are less than 0.05 eV/Å (1 eV = 1.60 × 10⁻¹⁹ J).

The adsorption energy (E_a) is calculated by Eq. (1):

$$E_a = E_{\text{tot}} - E_{\text{CNT}} - E_{\text{mol}} \quad (1)$$

where E_{tot} and E_{CNT} are the total energies of B-doped (14,0) CNTs with and without the molecules, respectively, and E_{mol} is the total energy of an isolated molecule.

To obtain quantum transport properties, the scattering wave functions of the B-doped (14,0) CNTs with and without molecules sandwiched between two semi-infinite B-doped (14,0) CNTs are calculated based on the overbridging boundary-matching (OBM) method [29-32]. For the calculation of the scattering wave functions, the real-space finite-difference approach is employed [33,34], and the grid spacings are taken to be 0.24 Å which corresponds to the cutoff energy of 46.8 Ry. The

conductance $G(E)$ is calculated from the transmission coefficients $T_i(E)$ through the Landauer-Büttiker formula (2) [35]:

$$G(E) = \frac{2e^2}{h} \sum_i T_i(E) \quad (2)$$

where i is the number of electron channels, and e and h denote the electron charge and the Planck constant, respectively.

The STM images are obtained based on the Tersoff-Hamann (TH) approach [36], and the TH method is known to be valid for many systems despite its simplicity [37]. In this approach, the tunneling current $I(r)$ is approximated to be proportional to the local density of states (LDOS) of the surface at the tip position integrated over a range of energy restricted by the applied bias voltage V , *i.e.*

$$I(r) \sim \int_{E_F}^{E_F+eV} \rho(r, \varepsilon) d\varepsilon \quad (3)$$

where E_F denotes the Fermi energy. The images obtained with negative and positive voltages reflect the occupied and unoccupied electronic states, respectively [38,39].

Results and discussion

Atomic structures and energetics

We here study the atomic structures of B-doped zigzag (14,0) CNTs without the adsorbed molecules. Unlike graphene, the zigzag carbon nanotubes have two kinds of C-C bonds around each atom. The two kinds of the B-C bond lengths of B-doped (14,0) CNT are found to be 1.46 and 1.49 Å, and are considerably longer than two kinds of the C-C bond lengths (1.40 and 1.41 Å) in a pristine (14,0) CNT. In addition, the two kinds of B-C bond lengths are longer and shorter, compared with that of B-doped graphene (1.47 Å) [40,41].

Table 1. Adsorption energy E_a and binding distance d from B atom for each molecule adsorbed on B-doped (14,0) CNTs

	CO	CO ₂	O ₂	N ₂
E_a / eV	-0.30	-0.01	-0.20	-0.21
d / Å	1.54	2.62	1.66	3.37

We also study the adsorption properties of molecules, including environmentally toxic molecules on the B-doped (14,0) CNTs. Table 1 shows the adsorption energy and the binding distance between the molecule and the B atom in the B-doped (14,0) CNTs, and the optimized atomic configurations of CO and O₂ molecules adsorbed on B-doped (14,0) CNTs are shown in Fig. 1. It is found that the CO and O₂ molecules are adsorbed with relatively large adsorption energies and short binding distances. It is also found that the B atoms in the B-doped CNTs protrude from the tube surface when CO and O₂ molecules are adsorbed on the B-doped CNTs [Figs. 1(a) and 1(b)]. On the other hand, the CO₂ and N₂ molecules weakly bind with relatively small adsorption energy as well as long binding distances. The adsorption energy of the CO molecule on the B-doped (14,0) CNT is much smaller and larger than those on the B-doped (8,0) CNT and the B-doped graphene, respectively. Thus, the adsorption energy would diminish as the tube diameter increases, and it is expected that the curvature of the nanotubes could improve the chemical reactivity to the adsorbates [8,10,21].

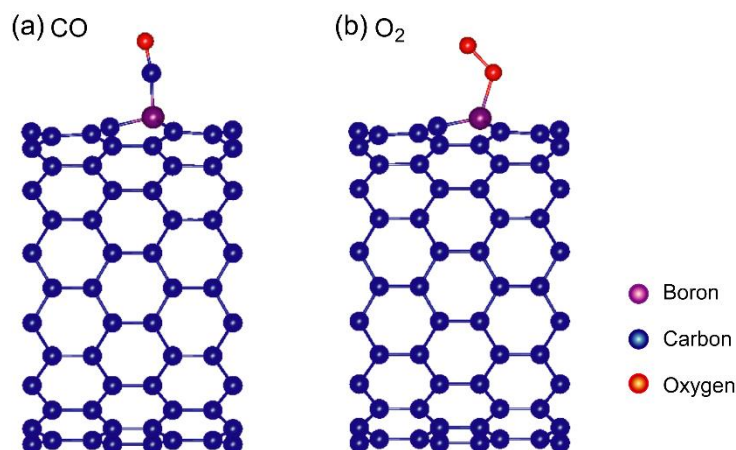


Figure 1. Optimized structures of (a) CO and (b) O₂ molecules on B-doped (14,0) CNTs

Scanning tunneling microscopy

Scanning tunneling microscopy (STM) is one of the most effective methods to observe the local electronic structures of the surfaces at atomic levels [40,41]. Figure 2 shows the STM images of B-doped (14,0) CNTs with and without CO and O₂ molecules. One finds that there is a triangle-shaped hillock around the B atom in the B-doped CNT [Fig. 2(a)]. It is also observed theoretically and experimentally in the B-doped graphene [17,41,42]. When the CO molecule is adsorbed on the B-doped CNT, one can find that the gourd-shaped corrugation above the CO molecule appears [Fig. 2(b)]. On the other hand, there are two ring-like corrugations above the O₂ molecule in the STM image when O₂ molecule is adsorbed [Fig. 2(c)]. In addition, it is interesting that the STM images at the bias voltages of +0.5 and -0.5 V are different from each other. Thus, the B atom and the CO molecule as well as the O₂ molecule can be clearly identified in the STM images of B-doped (14,0) CNTs.

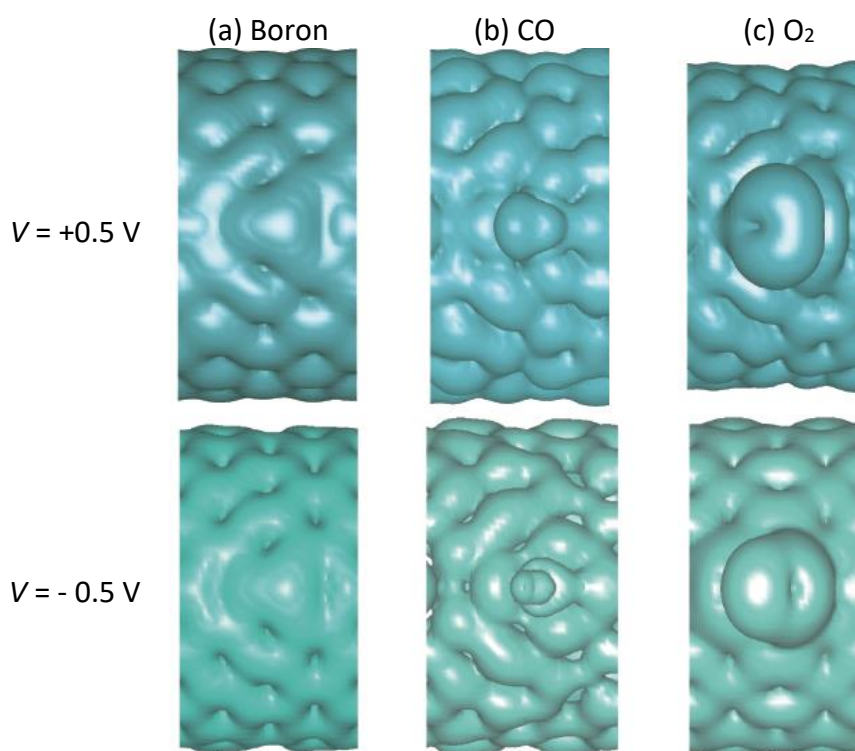


Figure 2. Scanning tunneling microscopy of B-doped (14,0) CNTs: (a) without any adsorbates; (b) with CO molecule; (c) with O₂ molecule. STM images are generated at bias voltages of +0.5 V (upper panel) and -0.5 V (lower panel)

Quantum transport properties

We examine how the quantum transport of (14,0) CNTs is affected by the introduction of the B atom and the adsorption of molecules. Figure 3 exhibits the quantum conductance $G(E)$ of the (14,0) CNTs as a function of energy E . The (14,0) CNT shows a semiconducting property with a band gap of ~ 0.46 eV. The pristine CNT possesses quantized conductance and step-like structures, as shown in the black lines of Figure 3. One finds that the pristine (14,0) CNT has the conductance of $2G_0$ near the valence-band and the conduction-band edges, where $G_0=2e^2/h$ is the unit of the quantum conductance. Interestingly, the conductance spectrum of the (14,0) CNT shows the symmetric behavior, whereas that of the (8,0) CNT possesses an asymmetric one: In the valence-band edge, both of the (14,0) and (8,0) CNTs have $2G_0$, while the (14,0) CNT has $2G_0$ and the (8,0) CNT has $1G_0$ in the conduction-band edge [8].

Introduction of the B atom into the semiconducting CNTs induces the acceptor states near the valence-band edge, and therefore the Fermi level of the B-doped (14,0) CNT relatively moves toward the valence bands. As a result, the B-doped (14,0) CNT shows a *p*-type semiconducting property [see Fig. 3]. When a CO molecule is adsorbed on the B-dopant atom in the B-doped (14,0) CNT, one can find that the conductance spectrum largely changes: the adsorption of the CO molecule overall reduces the conductance of the B-doped CNTs, while the conductance of the B-doped (14,0) CNT is quantized. In the case of the adsorption of the O₂ molecule, the conductance spectrum shows similar behaviors to that for the adsorption of the CO molecule, but the slopes of both conductance spectra from $E = 0$ to -0.5 eV are different from each other. Figures 4(a) and 4(b) show the scattering wave functions at the Fermi energy for the adsorption of the CO molecule and the O₂ molecule, respectively. The B-doped (14,0) CNT has two conduction channels at the Fermi energy, as already discussed [see Fig. 3]. When the CO molecule is adsorbed, electrons in one of two conduction channels are almost scattered and therefore, its scattering wave function is localized around the CO molecule, and the other is composed of the delocalized π -orbital state [Fig. 4(a)]. For the adsorption of the O₂ molecule, one of two conduction channels is almost localized around the O₂ molecule and the other is the extending π -orbital state as well [Fig. 4(b)].

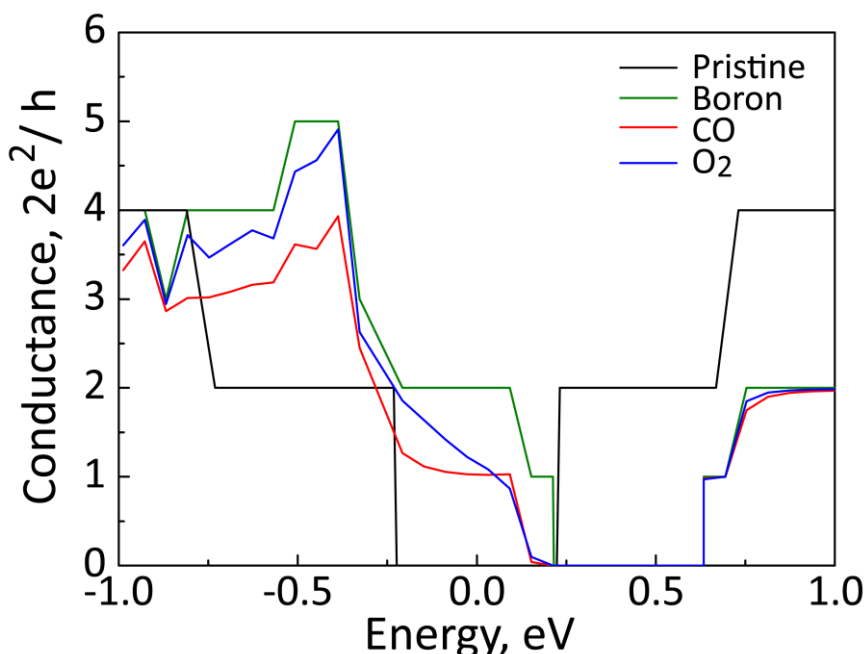


Figure 3. Quantum conductance of pristine (14,0) CNT and B-doped (14,0) CNT without any adsorbates, and with CO and O₂ molecules

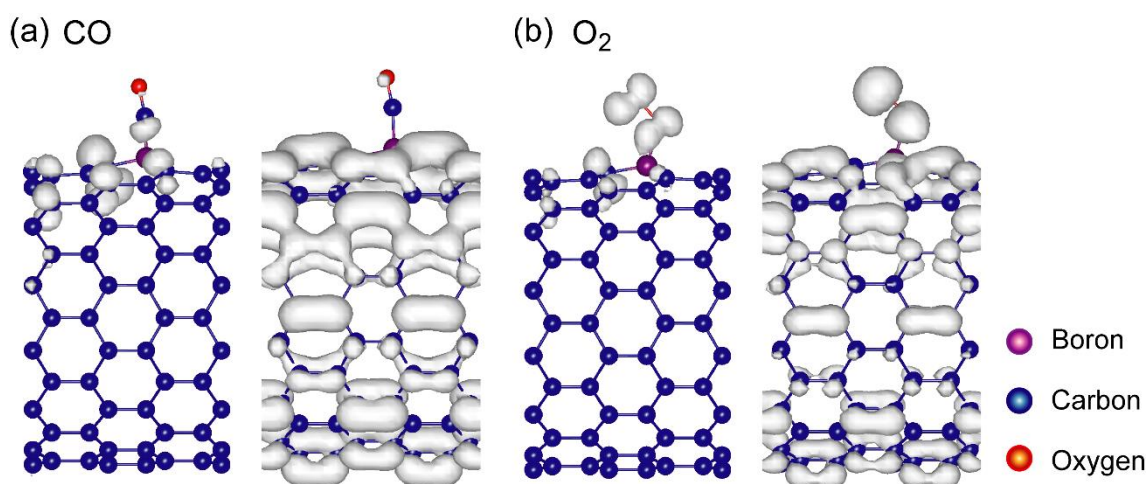


Figure 4. Iso-surfaces of squared scattering wave functions of B-doped (14,0) CNT with (a) CO molecule and (b) O₂ molecule at the Fermi energy

We now discuss the sensitivity of CNT-based molecular sensors and define the changes $\Delta G(E) / \% = ((G_a - G_b) / G_b) \times 100$, where G_a and G_b are the conductance of the B-doped (14,0) CNT with and without molecules, respectively. Table 2 shows the conductance change $\Delta G(0)$ at the Fermi energy ($E = 0$ eV). The changes $\Delta G(E = 0)$ for the adsorption of the CO molecule and the O₂ molecule are -48.6 and -38.8 %, respectively. It is therefore found that the CO and O₂ molecules adsorbed on the B-doped CNT are distinguishable without any applied bias voltages.

Table 2. Changes in the conductance at the Fermi energy [$\Delta G(0)$] for the adsorption of CO and O₂ molecules on the B-doped (14,0) CNT. The changes in the conductance are calculated with respect to the B-doped (14,0) CNT

	CO	O ₂
$\Delta G(0) / \%$	-48.6	-38.8

Conclusions

The effects of doping and adsorption of molecules on atomic structures, energetics, and quantum transport of B-doped (14,0) CNTs have been studied based on our first-principles electronic structure and quantum transport studies. The CO and O₂ molecules are adsorbed on the B-doped CNTs with relatively large adsorption energies, while CO₂ and N₂ molecules are weakly adsorbed with long binding distances. The quantum conductance of (14,0) CNTs regarding the adsorption of the molecules is examined. The introduction of the dopant atom and the adsorption of the molecules are found to sizably vary the quantum conductance of the CNTs. The nature of the variation of the quantum conductance induced by the doping and the adsorption of the molecules is clarified in terms of the spatial distributions of the scattering wave functions and the possibility to selectively detect toxic CO molecule and common O₂ molecule in the air are discussed. The B-doped CNT could selectively detect toxic CO molecules and common O₂ molecules under low bias voltages.

Acknowledgements: This work was partly supported by JSPS KAKENHI Grant Numbers JP17K05053 and JP21K04876. Computations were partly done at Institute for Solid State Physics, the University of Tokyo.

References

- [1] S. Iijima, *Nature* **354** (1991) 56-58. <https://doi.org/10.1038/354056a0>

- [2] T. Dürkop, S. A. Getty, E. Cobas, M. S. Fuhrer, *Nano Letters* **4** (2004) 35-39. <https://doi.org/10.1021/nl0491475>
- [3] P. G. Collins, K. Bradley, M. Ishigami, A. Zettl, *Science* **287** (2000) 1801-1804. <https://doi.org/10.1126/science.287.5459.1801>
- [4] J. Kong, N. R. Franklin, C. W. Zhou, M. G. Chapline, S. Peng, K. J. Cho, H. J. Dai, *Science* **287** (2000) 622-625. <https://doi.org/10.1126/science.287.5453.622>
- [5] D. R. Kauffman, C. M. Shade, H. Uh, S. Petoud, A. Star, *Nature Chemistry* **1** (2009) 500-506. <https://doi.org/10.1038/nchem.323>
- [6] S. Sorgenfrei, C. Chiu, R. L. Gonzalez, Y.-J. Yu, P. Kim, C. Nuckolls, K. L. Shepard, *Nature Nanotechnology* **6** (2011) 126-132. <https://doi.org/10.1038/nnano.2010.275>
- [7] R. Peng, X. S. Tang, D. Li, *Small* **14** (2018) 1800013. <https://doi.org/10.1002/sml.201800013>
- [8] Y. Fujimoto, S. Saito, *Applied Surface Science Advances* **1** (2020) 100028. <https://doi.org/10.1016/j.apsadv.2020.100028>
- [9] Y. Fujimoto, *Modern Physics Letters B* **35** (2021) 2130001. <https://doi.org/10.1142/S0217984921300015>
- [10] Y. Fujimoto, S. Saito, *Japanese Journal of Applied Physics* **58** (2019) 015005. <https://doi.org/10.7567/1347-4065/aaf227>
- [11] J. M. H. Kroes, F. Pietrucci, K. Chikkadi, C. Roman, C. Hierold, W. Andreoni, *Applied Physics Letters* **108** (2016) 033111. <https://doi.org/10.1063/1.4940422>
- [12] F. Schedin, A. K. Geim, S. V. Morozov, E. W. Hill, P. Blake, M. I. Katsnelson, K. S. Novoselov, *Nature Materials* **6** (2007) 652-655. <https://doi.org/10.1038/nmat1967>
- [13] S.-H. Jhi, S. G. Louie, M. L. Cohen, *Physical Review Letters* **85** (2000) 1710. <https://doi.org/10.1103/PhysRevLett.85.1710>
- [14] H. Chang, J. D. Lee, S. M. Lee, Y. H. Lee, *Applied Physics Letters* **79** (2001) 3863. <https://doi.org/10.1063/1.1424069>
- [15] N. Peng, Q. Zhang, C. L. Chow, O. K. Tan, N. Marzari, *Nano Letters* **9** (2009) 1626-1630. <https://doi.org/10.1021/nl803930w>
- [16] C. Gómez-Navarro, P. J. De Pablo, J. Gómez-Herrero, B. Biel, F. J. Garcia-Vidal, A. Rubio, F. Flores, *Nature Materials* **4** (2005) 534-539. <https://doi.org/10.1038/nmat1414>
- [17] Y. Fujimoto, S. Saito, *Chemical Physics* **478** (2016) 55-61. <https://doi.org/10.1016/j.chemphys.2016.05.014>
- [18] S. Peng, K. J. Cho, *Nano Letters* **3** (2003) 513-517. <https://doi.org/10.1021/nl034064u>
- [19] Y. Fujimoto, S. Saito, *Journal of the Ceramic Society of Japan* **124** (2016) 584-586. <https://doi.org/10.2109/jcersj2.15285>
- [20] L. Bai, Z. Zhou, *Carbon* **45** (2007) 2105. <https://doi.org/10.1016/j.carbon.2007.05.019>
- [21] Y. Fujimoto, S. Saito, *Journal of Applied Physics* **115** (2014) 153701. <https://doi.org/10.1063/1.4871465>
- [22] Z. Zanolli, J.-C. Charlier, *Physics Review B* **80** (2009) 155447. <https://doi.org/10.1103/PhysRevB.80.155447>
- [23] P. Hohenberg, W. Kohn, *Physical Review* **136** (1964) B864. <https://doi.org/10.1103/PhysRev.136.B864>
- [24] W. Kohn, L. J. Sham, *Physics Review* **140** (1965) A1133. <https://doi.org/10.1103/PhysRev.140.A1133>
- [25] D. M. Ceperley, B. J. Alder, *Physical Review Letters* **45** (1980) 566. <https://doi.org/10.1103/PhysRevLett.45.566>
- [26] J. P. Perdew, A. Zunger, *Physical Review B* **23** (1981) 5048. <https://doi.org/10.1103/PhysRevB.23.5048>
- [27] N. Troullier, J. L. Martins, *Physical Review B* **43** (1991) 1993. <https://doi.org/10.1103/PhysRevB.43.1993>

- [28] Computations have been performed using Tokyo Ab-initio Program Package (TAPP) which has been developed by a consortium initiated at the University of Tokyo: J. Yamauchi, M. Tsukada, S. Watanabe, O. Sugino, *Physical Review B* **54** (1996) 5586. <https://doi.org/10.1103/PhysRevB.54.5586>
- [29] Y. Fujimoto, K. Hirose, *Physical Review B* **67** (2003) 195315. <https://doi.org/10.1103/PhysRevB.67.195315>
- [30] Y. Fujimoto, Y. Asari, H. Kondo, J. Nara, T. Ohno, *Physical Review B* **72** (2005) 113407. <https://doi.org/10.1103/PhysRevB.72.113407>
- [31] Y. Fujimoto, K. Hirose, T. Ohno, *Surface Science* **586** (2005) 74-82. <https://doi.org/10.1016/j.susc.2005.05.001>
- [32] T. Ono, S. Tsukamoto, Y. Egami, Y. Fujimoto, *Journal of Physics: Condensed Matter* **23** (2011) 394203. <https://doi.org/10.1088/0953-8984/23/39/394203>
- [33] J. R. Chelikowsky, N. Troullier, Y. Saad, *Physical Review Letters* **72** (1994) 1240. <https://doi.org/10.1103/PhysRevLett.72.1240>
- [34] K. Hirose, T. Ono, Y. Fujimoto, and S. Tsukamoto, *First-Principles Calculations in Real-Space Formalism, Electronic Configurations and Transport Properties of Nanostructures*, Imperial College Press, London, United Kingdom, 2005.
- [35] M. Büttiker, Y. Imry, R. Landauer, S. Pinhas, *Physical Review B* **31** (1985) 6207. <https://doi.org/10.1103/PhysRevB.31.6207>
- [36] J. Tersoff, D. R. Hamann, *Physical Review B* **31** (1985) 805. <https://doi.org/10.1103/PhysRevB.31.805>
- [37] Y. Fujimoto, H. Okada, K. Inagaki, H. Goto, K. Endo, K. Hirose, *Japanese Journal of Applied Physics* **42** (2003) 5267-5268. <https://doi.org/10.1143/JJAP.42.5267>
- [38] H. Okada, Y. Fujimoto, K. Endo, K. Hirose, Y. Mori, *Physical Review B* **63** (2001) 195324. <https://doi.org/10.1103/PhysRevB.63.195324>
- [39] Y. Fujimoto, A. Oshiyama, *Physical Review B* **87** (2013) 075323. <https://doi.org/10.1103/PhysRevB.87.075323>
- [40] Y. Fujimoto, S. Saito, *Physical Review B* **84** (2011) 245446. <https://doi.org/10.1103/PhysRevB.84.245446>
- [41] Y. Fujimoto, S. Saito, *Surface Science* **634** (2015) 57-61. <https://doi.org/10.1016/j.susc.2014.11.013>
- [42] L. Zhao, M. Levendorf, S. Goncher, T. Schiros, L. Palova, A. Zabet-Khosousi, K. T. Rim, C. Gutierrez, D. Nordlund, C. Jaye, M. Hybertsen, D. Reichman, G. W. Flynn, J. Park, A. N. Pasupathy, *Nano Letters* **13** (2013) 4659. <https://doi.org/10.1021/nl401781d>